Electronic Supplementary Material (ESI) for Green Chemistry.

Supporting Information

Synthesis of Metal-Organic Frameworks in water at room temperature: Salts as linker sources

Manuel Sánchez-Sánchez[*,†], *Negash Getachew*[†,§], *Kenya Díaz*[†], *Manuel Díaz-García*[†], *Yonas Chebude*[§], *Isabel Díaz*[†,§]

[†]Instituto de Catálisis y Petroleoquímica, ICP-CSIC, C/Marie Curie, 2 28049, Madrid, Spain

[§]Chemistry Department, Addis Ababa University, Addis Ababa, Ethiopia.

1. Experimental details of the syntheses of MOF materials

Unless otherwise stated, all syntheses were carried out at room temperature (23 ºC) and in water as the unique solvent. The general procedure is quite simple. Two different clear aqueous solutions were prepared: (i) a solution of the metal salt; and (ii) a solution of the linker salt Na_2BDC (disodium terephthalate) or, alternatively, the protonated organic linker with the stoichiometric amount of NaOH necessary to deprotonate the functional groups of the organic linker involved in the formation of the MOF material.

a. MIL-53(Al)

MIL-53(Al) materials were prepared by two different methods. In the first one, a clear solution of 8.4 g (40 mmol) of disodiumterephthalate (Na_2BDC) in 57.6 g (3.2 mol) of H_2O was added dropwise over another clear solution formed by dissolving 30 g (80 mmol) of aluminum nitrate nanohydrate salt, $Al(NO_3)_3{\cdot}9H_2O$, in 57.6 g (3.2 mol) of H_2O under stirring at room temperature. Such addition provokes the immediate appearance of a white precipitate. The mixture was maintaining under stirring at room temperature for one week. A representative aliquot was collected at different reaction times: 4 h, 8 h, 24 h, 4 days and 7 days. The white precipitate of any aliquot was washed with distilled water repeatedly and dried at room temperature overnight.

Alternatively, in the second method, a clear solution of terephthalic acid (H_2BDC) and a double molar amount of NaOH was added over another clear solution of $Al(NO_3)_3$, maintaining the same molar ratios as those described in the first method. Washing and drying processes were carried as described above.

For comparison purposes, a conventional MIL-53(Al) material was prepared as described in bibliography.[1]

The three MIL-53(Al) materials were calcined at 330 ºC for 3 days in air atmosphere.

b. NH_2-MIL-53(Al)

An aqueous yellow solution (Solution 1) was prepared by dissolving in 3 mL of deionized H_2O (166 mmol): (i) the organic linker NH_2-H_2BDC (375.6 mg, 2.07 mmol), and (ii) a slight excess of NaOH (179 mg, 4.5 mmol) with respect the in principle required amount (4.14 mmol) in order to insure the whole and quick deprotonation of the carboxylic groups of the organic linker. A second solution (Solution 2) was prepared dissolving $AlCl_3·6H_2O$ (500 mg, 2.07 mmol) in 2 mL of deionized H_2O. Solution 2 was dropwise added over Solution 1 under stirring, leading to the immediate appearance of a yellow solid, which became a gel-like mixture along the reaction time. After 24 hours of stirring at room temperature, the yellow solid was recovered from the mixture of pH=3.8 by centrifugation, and it was washed with deionized water several times.

For comparison purposes, a conventional NH_2-MIL-53(Al) material was prepared as described in bibliography.[2]

Both NH_2-MIL-53(Al) materials were treated with DMF at 150 ºC, as described elsewhere,[2] in order to remove any possible NH_2-H_2BDC filling the pores of the MOF structure.

c. NO_2-MIL-53(Al)

Taking the molar composition of the mixture from literature,[3] we applied the method as above. The chemicals (and their amounts) used were: organic linker NO_2-H_2BDC (0.92g, 4.36 mmol), H_2O (25 mL, 1.388 mol), NaOH (0.39 g, 9.79 mmol) for Solution 1; and $Al(NO_3)_3·9H_2O$ (1.49 g, 3.97 mmol) y H_2O (25 mL, 1.388 mol) for Solution 2. Order of addition, synthesis time, and the rest of experimental details were exactly equal to those described for NH_2-MIL-53(Al) materials. The resultant white solid did not immediately appear but the clear solution is slowly transformed into a suspension. The reaction was stopped after 24 hours.

For comparison purposes, a conventional NO_2-MIL-53(Al) material was prepared as described in bibliography.[3]

d. MOF-74

2,5-dihydroterephthalic acid (dhtp) (0.3 g, 1.51 mmol) was dissolved in an aqueous NaOH solution (4.954 g 1M, 4.76 mmol) (Solution 1). On the other hand, $Zn(CH_3COO)_2{\cdot}2H_2O$ (0.754 g, 3.4 mmol) was dissolved in 10 g of deionized water (Solution 2). Solution 2 was added dropwise over Solution 1 under stirring (150 rpm) and maintained for 20 hours under stirring. The solid was recovered by centrifugation, washed with water (20 mL) and then with methanol (20 mL). Afterwards, it was kept immersed in methanol for 6 days; that solvent was changed for the same amount of fresh methanol three times.

For comparison purposes, two MOF-74 materials were prepared as described in bibliography, one of them under conventional solvothermal conditions[4] and the second at room temperature using DMF as solvent.[5,6]

e. MOF-5

Two different syntheses of MOF-5 materials were carried out starting from Na_2BDC as linker source and both with DMF as solvent. The main difference between them was the synthesis temperature: room temperature or 100 ºC. Both processes were independently optimized, so the final ratio between reactants resulted quite different. In the synthesis of MOF-5 at room temperature, 4.39 g of $Zn(NO_3)_2{\cdot}6H_2O$ (14.76 mmol) was dissolved in 55.5 g of DMF, and 0.43 g of Na_2BDC (2.05 mmol), was dissolved in other 55.5 g of DMF. The metal salt solution was added to the linker solution under continuous stirring and the resulting solution was stirred for 24 h. The powder obtained was filtered and washed with DMF repeatedly. The product was dried on air over 24 h.

For the high temperature synthesis of MOF-5, 12.08 g of $Zn(NO_3)_2{\cdot}6H_2O$ (40.61 mmol) was dissolved in 55.5 g of DMF, whereas 0.86 g of Na_2BDC (4.10 mmol) was independently dissolved in other 55.5 g of DMF. The former solution was added to the latter under continuous stirring and the resulting solution was placed in an oven at 100 º C for 24 h. The powder obtained was allowed to cool to room temperature, filtered and washed with DMF repeatedly. The white precipitate formed was dried in air over 24 h.

For comparison purposes, two MOF-5 materials were prepared with H_2BDC as linker source and with DMF as solvent, following the most popular and conventional methods of the literature, that of the so-called IRMOF-1 material under solvothermal conditions[7] and that of the so-called MOCP-L material at room temperature.[8] In particular, both were prepared following the recipes described elsewhere.[9]

2. Nanocrystalline MIL-53(Al) prepared at room temperature starting from Na_2BDC

a. Crystal size estimation of the as-prepared MIL-53(Al) material

The ‘nano’ character of the MIL-53(Al) samples is manifest from the broadening of their XRD peaks compared to these of the conventional sample (Figure 1 of the main text). Although high-resolution microscopy techniques can in principle provide direct measurements of crystal size, the trend of the crystals to be agglomerated in larger particles, in which the crystals could be fused at some extent (Figure 2), makes difficult to accurately determine the crystal size by either TEM or SEM.[6]

In this context, the estimation of crystal size from PXRD peak broadenings could provide valuable information. Nevertheless, we are aware of the limitations of these methods,[10,11] particularly when the broadening of the XRD peaks is so high that it makes hard to find the required peaks with enough resolution to apply the more complete and precise methods. In any case, the application of the Scherrer's equation is always an acceptable option, especially if the samples are of nano-size and different reflections with well-represented Miller indices contribute to the analysis. Nevertheless, only one dimension (one value) of the crystals is obtained by applying this equation. With these criterions in mind, together with avoiding the overlapping with other reflections and choosing relatively intense reflections, the four peaks indicated in Figure S1 were selected.

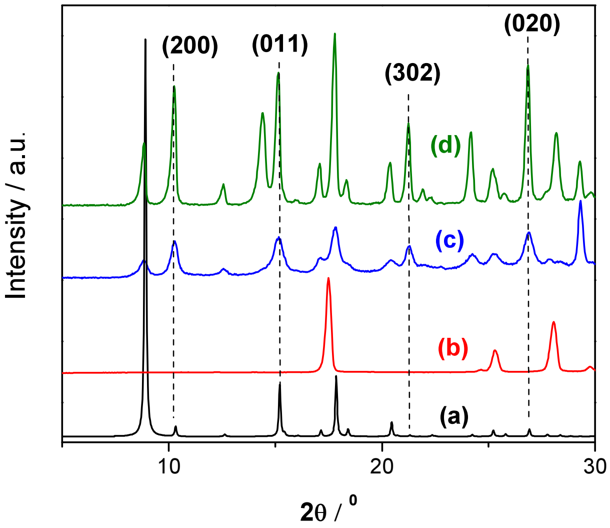

Figure S1. 5-30º region of the powder XRD patterns of different samples, clarifying the reflections selected for estimating crystal size by the application of the Scherrer's equation. (a) Theoretical pattern of an as-prepared MIL-53(Al) generated from data in the literature.[1] (b) Experimental pattern of the protonated linker 1,4-terephtalic acid (Aldrich). (c) Experimental XRD patterns of an as-prepared MIL-53(Al) sample in water and room temperature. (d) Experimental pattern of an as-prepared MIL-53(Al) sample prepared according to the original recipe.[1] Vertical dashed black lines indicate the 2Θ positions of the selected reflections, whose Miller indices are indicated at the top.

Scherrer equation[12] is the most extended method for estimating the crystal size from powder XRD peaks broadenings. The mathematical expression of the Scherrer's equation is:

$$\beta_S\,(2\theta)_{hkl} = \frac{K\lambda}{T\cos\theta_{hkl}}$$

where β_S is the crystal size contribution to the peak width in radians (in our case, calculated from FWHM after subtracting the instrumental broadening $FWHM_{inst}$ measured from the same XRD reflections of the large-crystal Zn-MOF-74 prepared at high temperature, assuming a Gaussian shape of the XRD peaks: $\beta_S\ (2\theta)_{hkl} = \sqrt{(FWHM)^2 - (FWHM_{inst})^2}$), K is a constant near unity (we have taken a k value of 0.9, as it is a good approximation when β_S is taken as FWHM, the full width at half maximum), λ is the wavelength of the X-ray radiation in nm (in our case, 0.15418 nm) and T is the average thickness of the crystal in a direction normal to the diffracting plane hkl.

Table S1 summarizes the Scherrer-based crystal size estimation process of the samples whose XRD patterns are shown in Figure 1 of the main text. As explained in the main text, the solid immediately formed once aluminum and BDC solutions were mixed is very rich in H_2BDC phase, but it also contains some MIL-53(Al). The latter increases to the detriment of the former so that the already-formed MIL-53(Al) nanocrystals continue growing during the formation of MOF as H_2BDC disappears.

Table S1. Data of crystal size estimation by applying the Scherrer's equation to the different MIL-53(Al) samples whose XRD patterns are included in Figure 1a of the main text. These samples were prepared at room temperature using Na_2BDC as linker source and from a unique batch, with the reaction time being the only difference among them.

Sample	Reflection hkl	FWHM / º	$\beta_S\ (2\theta)_{hkl}$ / rad	cos Θ_{hkl}	T_{hkl} / nm	Crystal size / nm
MIL-53(Al)-4h	200	0.45	0.00773	0.9838	18.23	**16.2**
	011	na[a]	na[a]	0,9649	na[a]	
	302	0.61	0.01050	0.9318	14.17	
	020	na[a]	na[a]	0.8918	na[a]	
MIL-53(Al)-8h	200	0.30	0.00505	0.9838	27.93	**20.6**
	011	0.53	0.00912	0.9649	15.76	
	302	0.42	0.00712	0.9318	20.90	
	020	0.51	0.00865	0.8918	17.97	
MIL-53(Al)-24h	200	0.29	0.00487	0.9838	28.97	**21.6**
	011	0.50	0.00858	0.9649	16.74	
	302	0.38	0.00640	0.9318	23.26	
	020	0.53	0.00901	0.8918	17.26	
MIL-53(Al)-4d	200	0.22	0.00358	0.9838	39.40	**27.7**
	011	0.44	0.00752	0.9649	19.12	
	302	0.31	0.00512	0.9318	29.06	
	020	0.40	0.00666	0.8918	23.36	
MIL-53(Al)-7d	200	0.22	0.00358	0.9838	39.40	**28.5**
	011	0.41	0.00698	0.9649	20.58	
	302	0.30	0.00494	0.9318	30.14	
	020	0.39	0.00648	0.8918	24.00	

[a] Width of the reflections 011 and 020 could not be measured with enough accuracy in the sample MIL-53(Al)-4h due to either their low intensity or a significant overlap with an intense reflection of the protonated linker.

Since MIL-53(Al) material is not mainly formed immediately after mixing both solutions, it makes sense to study its formation at different synthesis temperatures. Figure 1 of the main text and Table S2 summarizes the results in terms of the obtained phase. With enough crystallization time for each case, MIL-53(Al) could be purely achieved. The crystal size increases with temperature, probably because crystalline growth is favored at high temperature against the formation of new nuclei. As a consequence, the synthesis temperature rather than the synthesis procedure seems to be the key factor to give a particular crystal size. Nevertheless, the method based on the linker salt approach provides MIL-53(Al) samples with smaller crystal size than the conventional method even at the same temperature, probably due to the nucleation that takes place at some extent in the former case, even at room temperature.

Table S2. Data of crystal size estimation by applying the Scherrer's equation to the different MIL-53(Al) samples whose XRD patterns are included in Figure 1b of the main text. These samples were prepared at different temperatures using Na_2BDC as linker source and at 220 ºC following the conventional method.[1]

Method-T	Reflection hkl	FWHM / º	$\beta_S\ (2\theta)_{hkl}$ / rad	cos Θ_{hkl}	T_{hkl} / nm	Crystal size / nm
Convent.[1]- 220 ºC	200	0.09	0.00072	0.9838	195.85	**92.7**
	011	0.14	0.00187	0.9649	76.77	
	302	0.19	0.00282	0.9318	52.77	
	020	0.23	0.00342	0.8918	45.40	
This work- 220 ºC	200	0.13	0.00179	0.9838	78.80	**61.6**
	011	0.16	0.00231	0.9649	62.24	
	302	0.18	0.00261	0.9318	56.96	
	020	0.22	0.00322	0.8918	48.31	
This work- 150 ºC	200	0.21	0.00339	0.9838	41.59	**35.3**
	011	0.23	0.00369	0.9649	38.90	
	302	0.28	0.00456	0.9318	32.60	
	020	0.34	0.00555	0.8918	28.00	
This work- 75 ºC	200	0.21	0.00339	0.9838	41.59	**29.7**
	011	0.37	0.00626	0.9649	22.94	
	302	0.30	0.00494	0.9318	30.14	
	020	0.39	0.00648	0.8918	24.00	
This work- RT	200	0.22	0.00358	0.9838	39.40	**27.7**
	011	0.44	0.00752	0.9649	19.12	
	302	0.31	0.00512	0.9318	29.06	
	020	0.40	0.00666	0.8918	23.36	

b. Evolution of TG profiles of the as-prepared MIL-53(Al) material at room temperature as a function of the reaction time

One of the most relevant distinctions of the RT-prepared MIL-53(Al) materials compared with the conventional ones is the lesser (or even null, in the case of NO_2-MIL-53(Al)) amount of the protonated linker found within the pores. Since Figure 1 of the main text makes clear an evident evolution of the amount of H_2BDC with the time, the kinetic following of these materials by TGA (Figure S3) is rather appropriate. At short reaction times (4 or 8 hours), the collected solid is widely dominated by the phase H_2BDC (Figures 1 and S3), whose TGA loss (below 350 ºC) is practically not affected by the minor amount of MIL-53(Al). After 24 hours of reaction, the MIL-53(Al) phase becomes dominant, and the remaining amount of H_2BDC is lost at temperatures (at *ca.* 410 ºC) higher than the free H_2BDC. Although the reasons of this increase in loss temperature are not completely clear, we think that H_2BDC could be encapsulated within the mesopores defined by the MIL-53(Al) nanocrystals agglomeration

(Figure 2 of the main text), what could retard the linker elimination. For prolonger times, the loss of H_2BDC continues being reduced in both amount and temperature, whereas the amount of water becomes important after 7 days of reaction time.

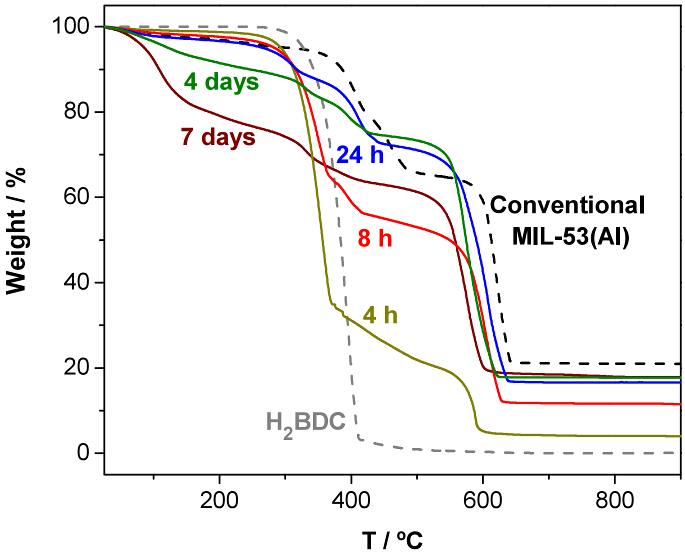

Figure S2. TG profiles of the different MIL-53(Al) samples prepared at room temperature in water with Na_2BDC as linker sources (solid lines), extracted after different reaction time. The TG profile of a conventional MIL-53(Al) material (dashed black line) and the free organic linker H_2BDC (dashed grey line) are also shown to make easier the interpretation of the losses of the RT-prepared MIL-53(Al) samples.

c. Calcination of the material: H_2BDC-free MIL-53(Al) material prepared at room temperature.

Due to the remarkable flexibility of the MIL-53(Al) materials, at least three different forms of this material can be isolated as a function of the chemical species inside of the pores.[1] These three forms are known as: (i) MIL-53(Al)-*as* corresponding to the as-prepared sample with H_2BDC molecules within the pores; (ii) MIL-53(Al)-*ht* (*ht* for high temperature) obtained when the as-prepared MIL-53(Al) is calcined and therefore its pores are free of any adsorbed molecule; and (iii) MIL-53(Al)-*lt* (*lt* for low temperature) that has some water molecules within the pores and that normally results from MIL-53(Al)-*ht* once it is exposed to the (humid) ambient.[1] MIL-53(Al)-*ht* and MIL-53(Al)-*lt* can be easily interconverted each other by the reversible presence/absence of water within the pores.

Figure S3 compares the XRD patterns of the MIL-53(Al) materials prepared at room temperature and using Na_2BDC as linker source and that of a conventional MIL-53(Al) material, both after being calcined at 330 ºC during 3 days under uncontrolled atmosphere and after being exposed for one week to the ambient condition. Unexpectedly, both patterns are markedly different. Whereas the conventional MIL-53(Al) behaves as described in the literature,[1] i.e. the calcination followed by exposure to the air basically leads to the hydrated MIL-53(Al)-*lt* form, the MIL-53(Al) material prepared at room temperature adopts the water-free MIL-53(Al)-*ht* form. In other words, the calcined RT-prepared MIL-53(Al) material is not hydrated, at least not immediately (its pattern did not neither change a couple of months after calcination, with no indication of the presence of MIL-53(Al)-*lt* form). This could have some implications for certain applications, since a dehydration process may not be required to evacuate its pores.

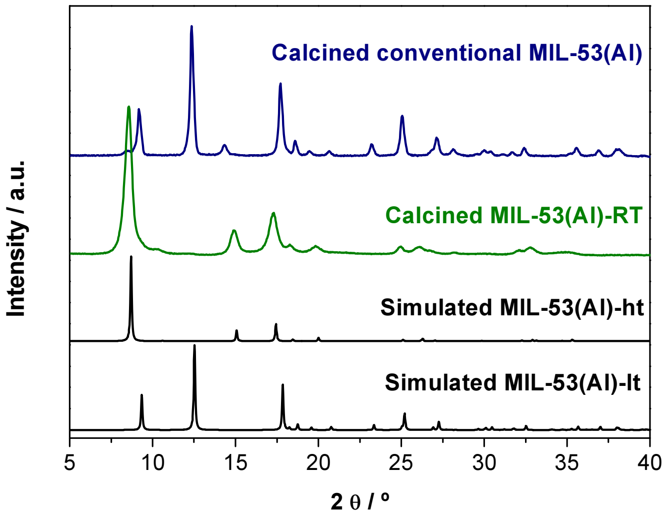

Figure S3. From the top to the bottom, experimental powder XRD pattern of a calcined MIL-53(Al) material prepared at room temperature (green line), experimental powder XRD pattern of a calcined MIL-53(Al) material prepared by conventional method (blue),[1] simulated pattern of MIL-53(Al) material in *ht* form (black), and simulated pattern of a MIL-53(Al) material in a *lt* form (black).

On the other hand, Figure 3 of the main text shows a significant difference between the isotherms of the conventional and the RT-prepared MIL-53(Al) materials in terms of N_2 adsorbed at high relative pressure p/p_0, due to the existence of a non-negligible external surface area in the RT sample, which is caused by the relatively ordered arrangements of nanocrystals. Obviously, this was also made clear by the pore size distribution (PSD) arising from these isotherms. Figure S4 shows the PSD profiles of the adsorption branches of both isotherms. The PSD profile of the conventional MIL-53(Al) is practically flat with no remarkable feature. On the contrary, the PSD profile of the MIL-53(Al)-RT has a broad peak with a maximum centered at 35.5 nm (21.3 nm is the maximum in the PSD desorption profile, obviously with much sharper distribution). This difference could become key for some applications, such as for heterogeneous catalysis, as the reactants and/or products diffusion will be favored in the case of the MIL-53(Al)-RT, in spite of the fact that the N_2 adsorption in the mesopore region is due to inter-crystalline mesoporosity.

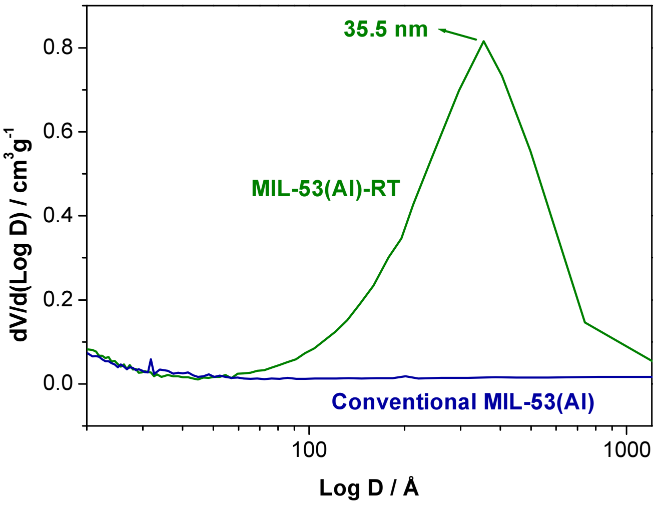

Figure S4. Pore side distribution (PSD) of the adsorption branches of the MIL-53(Al) materials prepared at room temperature (green line) and with conventional method (blue).

d. Nanocrystalline MIL-53(Al) prepared at room temperature starting from H_2BDC plus NaOH

Due to the scarce commercial availability of the linker salts, one may think that the here-reported method have limited applications. However, as Scheme 1 in the main text indicates, the formation of alkaline salts of organic linkers is straightforward from the corresponding (generally commercially-available) protonated source. The salt can be substituted by the protonated linker source plus the stoichiometric amount of a (strong) base (such as NaOH) necessary to deprotonate the carboxylic groups (for instance, NaOH/H_2BDC = 2). According to Scheme 1 shown in the main text, both options are chemically equivalent in water. Indeed, the isolation of the linker salt is not necessary when the solvent of the MOF formation is only water. If the solvent for the synthesis of MOF materials is not water, the salt can be equally formed in water and then isolated by rotavaporation as a previous step in the synthesis of the MOF materials.

Figure S5 shows the PXRD pattern of a MIL-53(Al) prepared at room temperature with an aqueous solution of H_2BDC and NaOH as organic linker source. For comparison purposes, the XRD patterns of both a MIL-53(Al) sample prepared at room temperature using Na_2BDC as linker source and a conventional MIL-53(Al) sample prepared at 220 ºC according to the literature,[1] are also shown. From a viewpoint of the phase nature, the resultant MIL-53(Al) sample is quite similar to that afforded at room temperature if the Na_2BDC salt was the source. The crystal size of this MIL-53(Al) material (estimated in 24.5 nm by Scherrer equation) is also quite similar to that of its homologue (see crystal size estimation as a function of synthesis time in Table S1).

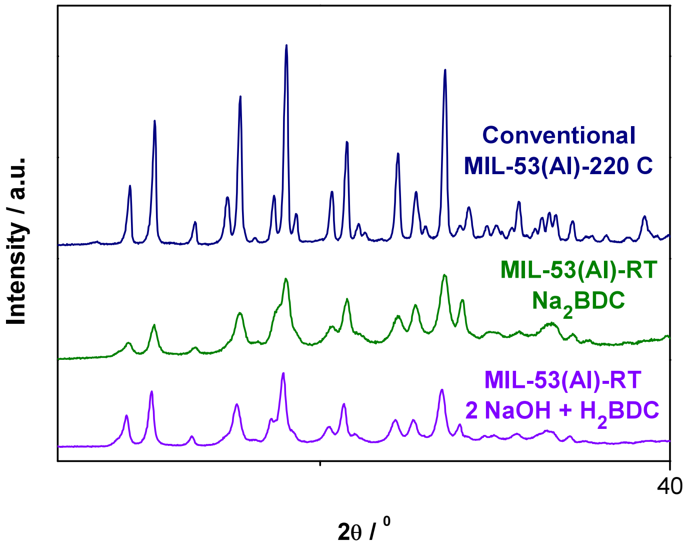

Figure S5. Powder XRD patterns of the two MIL-53(Al) samples prepared at room temperature, one of them using H_2BDC dissolved in NaOH solution as linker source (violet line, at the bottom), and the other one using Na_2BDC as organic linker source (green line, in the middle). At the top, the powder XRD pattern of a conventional MIL-53(Al) is also shown (blue line).

Apart from the nature of the phase, the textural properties of the resultant material are the other key factor to certify the possibility of affording a high-quality MIL-53(Al) material at room temperature. Figure S6 shows the N_2 adsorption/desorption isotherms at -196 ºC of the three MIIL-53(Al) samples whose PXRD patterns were shown in Figure S3. Like the other MIL-53(Al) sample prepared at room temperature, that prepared dissolving H_2BDC in a NaOH aqueous solution possesses textural properties only slightly lower than the conventional one, presumably because of its 'nano' nature.[6,13] Moreover, it has an extra contribution at higher partial pressure p/p_0 (in the limit of meso and macropores region) with a narrow hysteresis loop, probably due to the agglomeration of the nanocrystals in large particles containing some void intercrystalline space. In both total and external surface areas, the sample prepared with H_2BDC is even slightly better than its homologue prepared with Na_2BDC. On the contrary, the crystal size of the latter seems to be more homogenous than the former, according to the wider and better-defined hysteresis loop in the case of the isotherm of the MIL-53(Al) sample prepared from the salt linker.

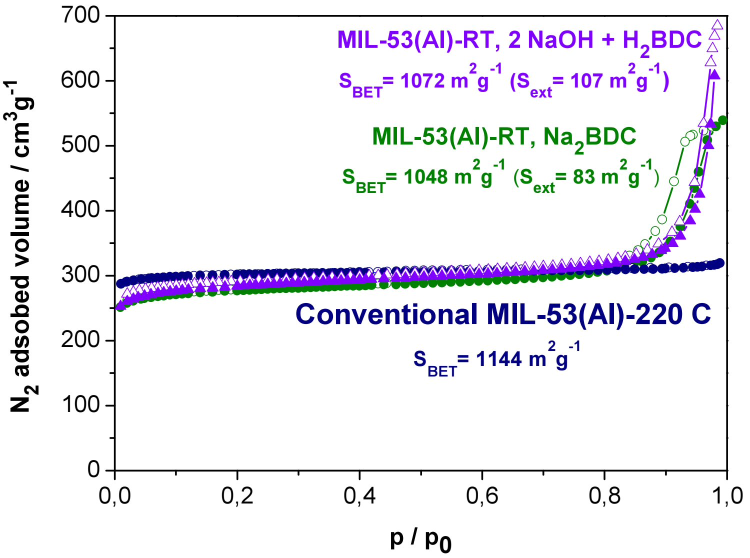

Figure S6. N_2 adsorption/desorption isotherms of the MIL-53(Al) prepared at room temperature with H_2BDC and NaOH (violet line)or with Na_2BDC (green), both at 220ºC following the conventional method.[1] The estimated surface area by applying BET method as well as the estimated external surface area by applying *t-plot* method, are indicated.

In summary, the use of H_2BDC and double moles of NaOH as BDC^{2-} source is basically equivalent to the use of Na_2BDC, what opens the possibility of extending the here-proposed method to any system in which the protonated organic linker is either commercially available or susceptible of being prepared in the lab.

3. Nanocrystalline NH_2-MIL-53(Al) material prepared at room temperature starting from NH_2-H_2BDC plus NaOH

Figure 5 of the main text makes clear the 'nano'-sized nature of the NH_2-MIL-53(Al) sample prepared at room temperature. A more direct proof of this nanocrystallinity can be obtained from electron microscopy studies. Figure S7 shows two SEM images of this sample. Such studies showed that the sample is morphologically homogeneous, so that only particles like these seen in Figure S7-top could be detected. Like the particles forming the non-functionalized MIL-53(Al) sample, those of the NH_2-MIL-53(Al) samples are also agglomerates/aggregates of nanocrystals. As inferred from Figure S7-bottom, the size of these nanocrystals is relatively homogenous, although it can be changed within the range 15-50 nm.

Nanocrystals agglomeration also seems to define some intercrystalline mesoporosity, what was also suggested from the hysteresis loop of the corresponding N_2 isotherms shown in Figure 6 of the main text. Although that intercrystalline mesoporosity is much worst-defined than that of the MIL-53(Al) material (Figures 3 and S6), it must be taking into account that the isotherm of the NH_2-MIL-53(Al) sample was registered after a relatively aggressive thermal treatment in DMF. Milder treatment, although less efficient in removing NH_2-H_2BDC molecules, led to samples whose N_2 isotherms showed more pronounced N_2 adsorption/desorpiton in the mesoporous region and a better-defined hysteresis loop.

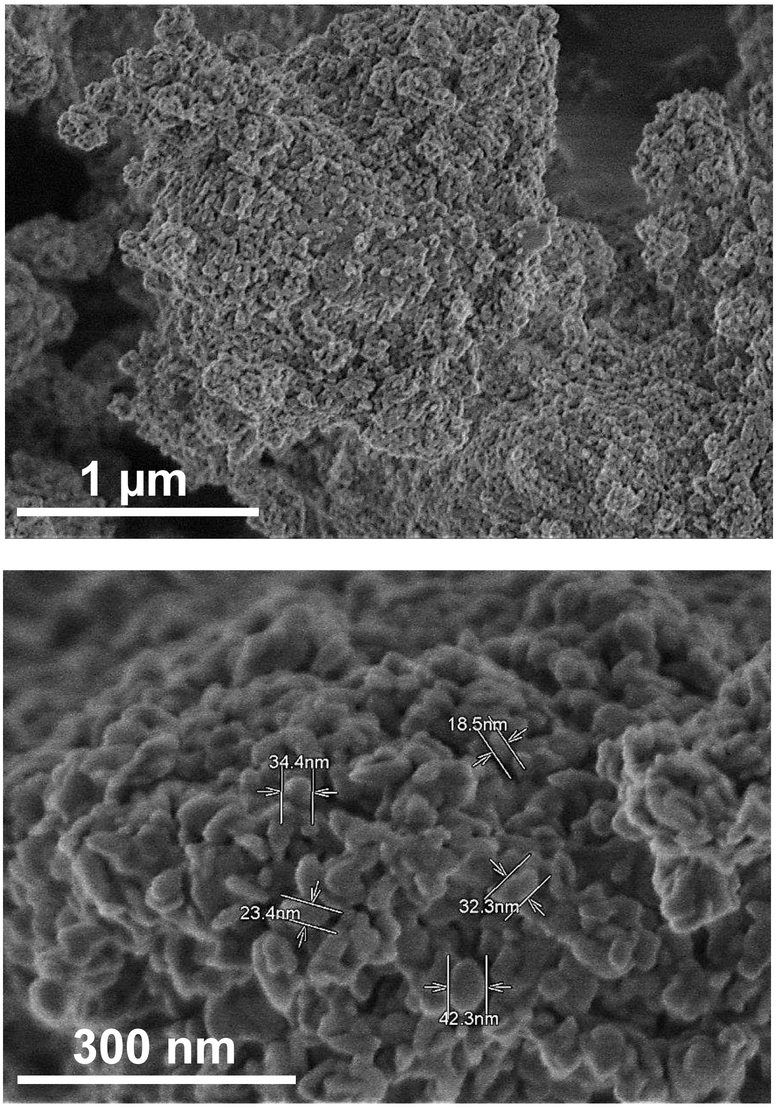

Figure S7. SEM micrographs of the NH_2-MIL-53(Al) sample prepared at room temperature at different magnifications. In the SEM micrograph at the bottom, the size of some dimension of a few crystals is indicated.

4. Nanocrystalline NO_2-MIL-53(Al) prepared at room temperature starting from NO_2-H_2BDC plus NaOH

Figure S8 shows the N_2 adsorption/desorption isotherm of the NO_2-MIL-53(Al) sample, which has been discussed in the main text.

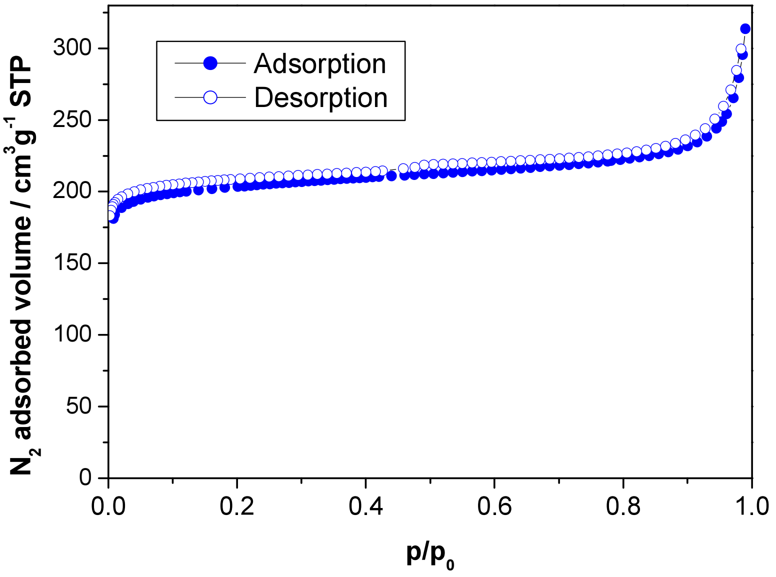

Figure S8. N_2 adsorption (full circles) /desorption (empty circles) isotherm of the NO_2-MIL-53(Al) sample prepared at room temperature in water, using an aqueous solution of NO_2-H_2BDC in presence of NaOH.

Unlike the isotherms of the non-functionalized and NH_2-functionalized MIL-53(Al), this isotherm does not have a significant contribution in the mesopore region. In addition, the sharp XRD peaks of its diffractogram (Figure 6-right) also suggest that the sample is formed by relatively large crystals. Figure S9 shows a couple of SEM micrographs of this sample. Effectively, the average crystal size of the NO_2-MIL-53(Al) sample is much larger than that found in their homologues MIL-53(Al) and NH_2-MIL-53(Al). Moreover, the plate-like shape of its crystals is very different from the round shape of the MIL-53(Al) crystals, which can easily agglomerate generating inter-crystalline mesoporosity.

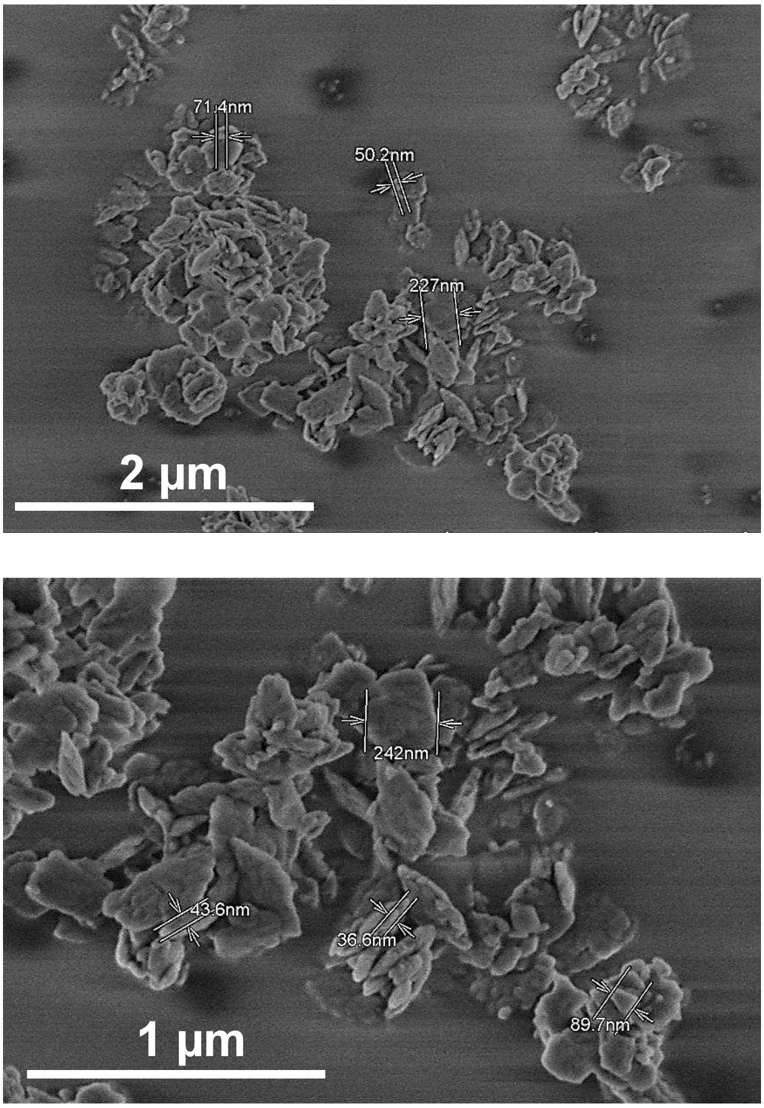

Figure S9. SEM images of the NO_2-MIL-53(Al) sample prepared at room temperature at different magnifications. The size of some dimension of a few crystals is indicated.

5. Zn-MOF-74 prepared at room temperature in water

In the main text, the section dedicated to the Zn-MOF-74 materials prepared in water focuses on a unique sample, whose preparation was optimized after several attempts. The process of that optimization can be illustrative in some aspects of the chemistry behind the formation of the MOFs materials in water at room temperature by using NaOH as linker deprotonating agent.

Table S3 shows some data of a series of attempts to prepare MOF-74 at room temperature and in water as unique solvent, in which only NaOH content of the mixture was systematically changed. Figure 10 shows the 5-20º region of the power XRD patterns of the resultant samples. The XRD pattern of the MOF-74 sample compared with the conventional MOF-74 samples in the main text is also included for comparison purposes but this sample does not belong to that systematic series of samples. In every pattern of the Figure S10, MOF-74 phase is present, and it is the main phase in all of them with the exception to the one prepared with a NaOH/dhtp ratio of 2.0 (bottom pattern in Figure S10). On the other hand, a crystalline impurity (becoming the main crystalline phase in the bottom XRD) is found in the XRD patterns of the samples prepared with NaOH/dhtp below 4. It is noteworthy to point out that four functional groups (two COOH and two OH) of the organic linker dhtp (2,5-dihydroxyterephthalic acid) have to be deprotonated to lead the formation of the MOF-74 material. In other words, beyond the need of generating a media that makes soluble dhtp, it seems to be essential to wholly deprotonate the functional groups of the organic linker that are involved in the formation of MOF-74 phase, in order to achieve it as the only crystalline phase.

Moreover, if the NaOH/dhtp ratio of the starting solution is higher than 4, an amorphous phase accompanies the Zn-MOF-74 phase. Such an amorphous phase, which is not evident in the region of XRD pattern selected in Figure S10 but it is directly seen at higher 2ϴ angles and deduced from its lower crystallinity, is maybe formed due to the precipitation of ZnO-based species. Supporting this interpretation, ZnO/$Zn(OH)_2$ species rather than soluble Zn^{2+} ones are the more thermodynamically-stable species at pH values higher than 5-8 (the pH range depends on the Zn concentration).[14]

Finally, the sample prepared under the optimal conditions of NaOH/dhtp ratio (= 4) is indeed a pure Zn-MOF-74 material. Nevertheless, this sample was not the best in terms of crystallinity, crystal homogeneity, etc., so it was optimized in different aspect until reaching the so-called optimized sample, which was formed from a starting mixture of 1 dhtp : 3.15 NaOH : 2.3 Zn : 367 H_2O. The list of changed parameters to reach that material is: NaOH/dhtp ratio of 3.15 instead of 4.0; Zn acetate dihydrate instead or Zn nitrate hexahidrate as Zn source, which compensates (at least partially) the lesser amount of the strong base NaOH in the mixture; 20 hours of reaction time instead of 4 hours used in the series of samples of Table S3; more concentrated system (H_2O/dhtp ratio of 367 instead of 600); higher Zn/dhtp of 2.3 instead of 2.0, following the trend of the recipes found in the literature.[4,15]

Table S3. Some experimental data of a series of synthesis attempts for preparing MOF-74 in water and at room temperature. The molar composition of the mixture was in all cases 1 dhtp : *x* NaOH : 2 Zn : 600 H_2O, where *x*, i.e. the NaOH/dhtp molar ratio, was varied from 2 to 5.

Experiment number	NaOH/dhtp	pH of the final mixture	Phases detected by PXRD
1	2.0	5.4	MOF-74 + unknown phase
2	2.5	5.6	MOF-74 + unknown phase
3	3.0	5.9	MOF-74 + unknown phase
4	4.0	7.2	MOF-74
5	5.0	9.7	MOF-74 + amorphous phase

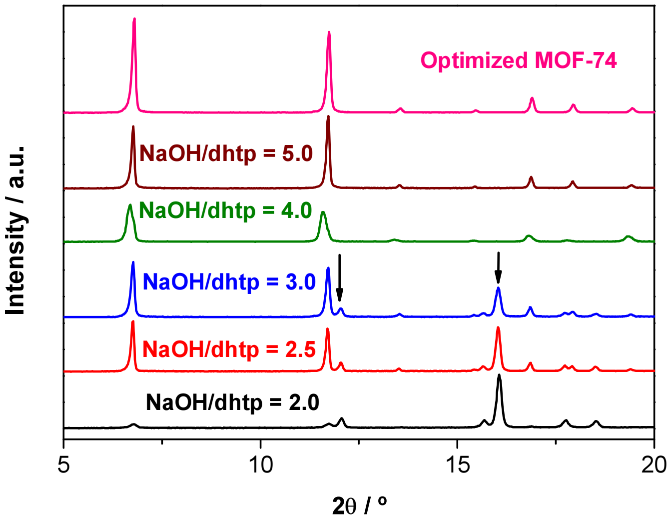

Figure S10. PXRD patterns of different MOF-74 samples prepared at room temperature in water. The optimized MOF-74 (magenta pattern) is the sample discussed in the main text. The other samples were systematically prepared from a general mixture of composition 1.0 dhtp : x NaOH : 2.0 Zn : 600 H_2O, only changing the NaOH/dhtp (x) ratio. The black arrows indicate the two most intense XRD reflections that do not belong to the pattern of the MOF-74 but to an unknown crystalline phase.

The sharp XRD reflections of the patterns of Figure S10, particularly these of the samples prepared under optimized synthesis conditions, indicate that Zn-MOF-74 samples are formed by large crystals. Figure S11 shows a couple of SEM micrographs of the optimized Zn-MOF-74 sample. (The low quality of these pictures is probably due to the fact that they were acquired using a Hitachi Tabletop TM-1000 microscope with very limited resolution). The samples are formed by crystalline particles. No particles with the appearance of amorphous phase could be identified. Resembling the typical morphology of the conventional MOF-74 samples,[15] the most abundant crystals have a slightly-elongated oblate shape with approximate dimensions of 1 x 3 µm, although the size distribution is not wholly homogeneous. Nevertheless, the homogeneity in both crystal shape and size is rather acceptable considering that they have been formed at room temperature and under magnetic stirring by adding dropwise a clear solution over another clear solution without strict control of addition speed.

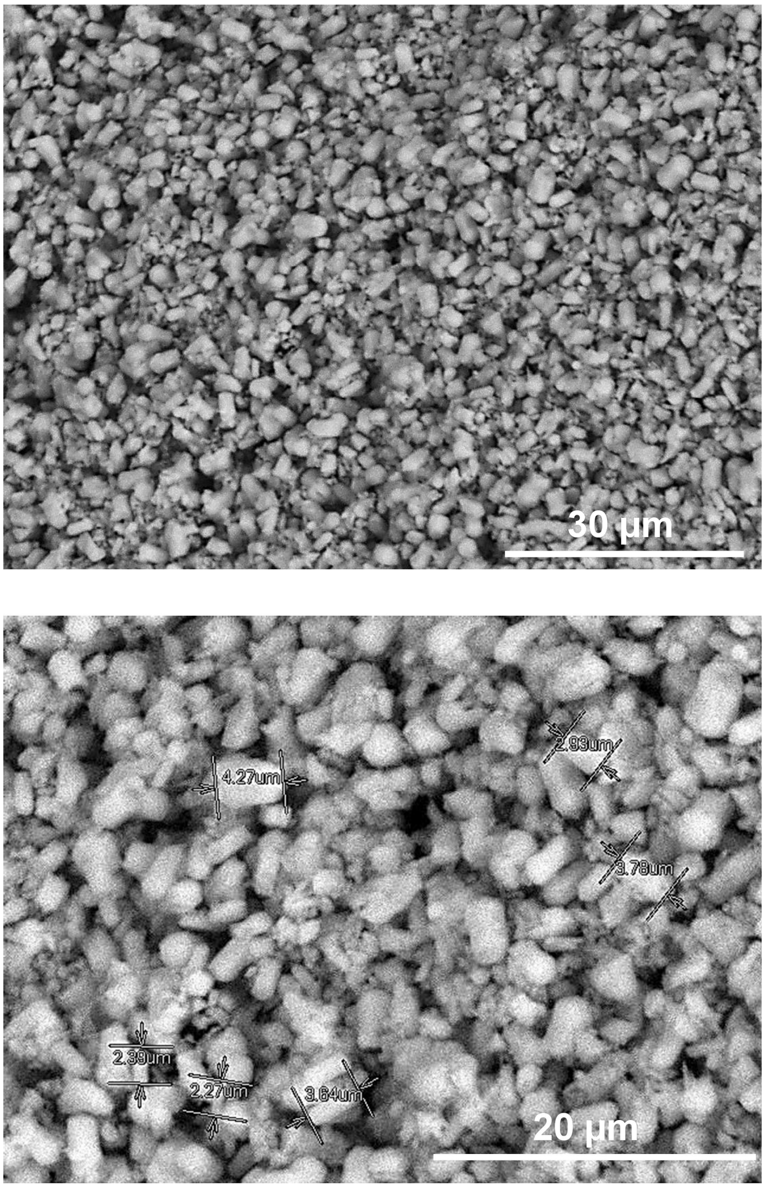

Figure S11. SEM images of the optimized MOF-74 sample prepared at room temperature at different magnifications. The size of some dimension of a few crystals is indicated in the image at the bottom.

6. MOF-5 materials prepared from Na_2BDC as linker source

It is well-known that changes in the synthesis conditions of MOF-5 provoke severe changes in the morphology of the resultant crystals.[9,16,17] The here-described method is different to any other reported so far, so the study of the morphology is pertinent. Figure S12 shows some SEM micrographs of the high-interpenetrated MOF-5 prepared with Na_2BDC at 100 ºC. The sample is formed by very large particles, sometimes larger than 100 µm. These samples are formed by a huge number of cubic crystals (which is the most typical shape of the MOF-5 prepared at high temperature)[9]. The size of the cube edge of these crystals is in the range 1-10 µm. Unlike the conventional IRMOF-1 material,[9] the crystals of this sample are not isolated and, indeed, they are not easily isolable. Instead, these crystals are partially fused as if not only the framework but also the crystals themselves are somehow interpenetrated to some extent.

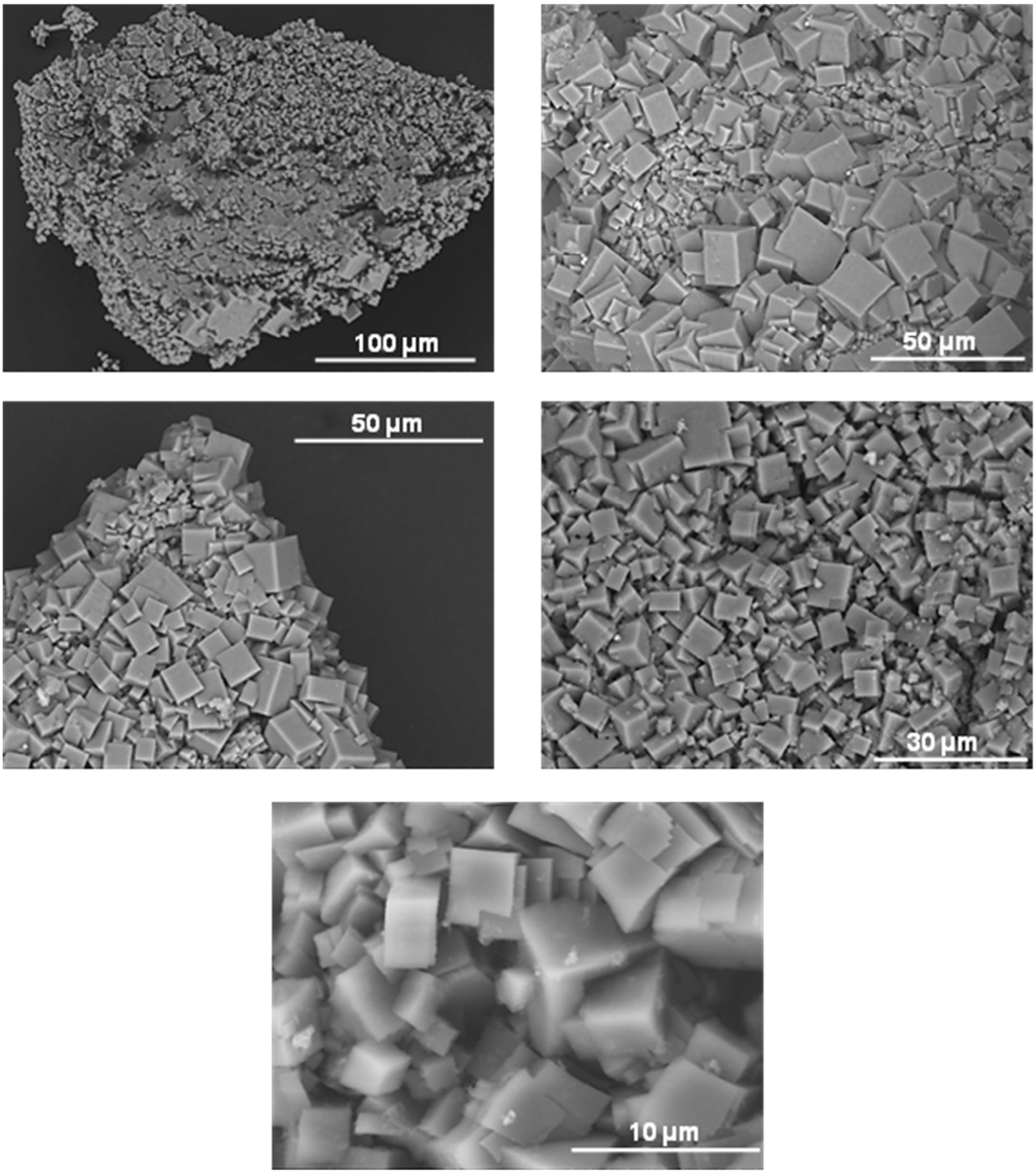

Figure S12. SEM micrographs at different magnification (from top to bottom, and to the left to the right: 800, 1500, 1800, 2500 and 9000) and of different zones of the sample highly-interpenetrated MOF-5 prepared at 100 ºC and using Na_2BDC as linker source.

Figure S13 shows some SEM micrographs of the MOF-5 material prepared with Na_2BDC at room temperature. The morphology of this material is markedly different to that of the homologous sample prepared at 100 ºC, just like it was observed between conventional MOF-

5 samples prepared at room or at high temperatures.[9] Nevertheless, both samples are formed by very large particles that contain some micrometer crystals. When the synthesis is carried out at room temperature, the crystals are smaller (as it could be foreseen from their broader XRD reflections of Figure 9 of the main text) and have not a very well-defined shape pattern. Some cubic-shape crystals seem to be present, somehow resembling the shape of the crystals of Figure S12. In any case, they are of irregular shape and they are accompanied by some other particles. At this point, it is noteworthy to remember that this sample is not a pure MOF-5 phase, but at least some other crystalline phase is present (Figure 9 o the main text), which could explain the crystal heterogeneity of this sample.

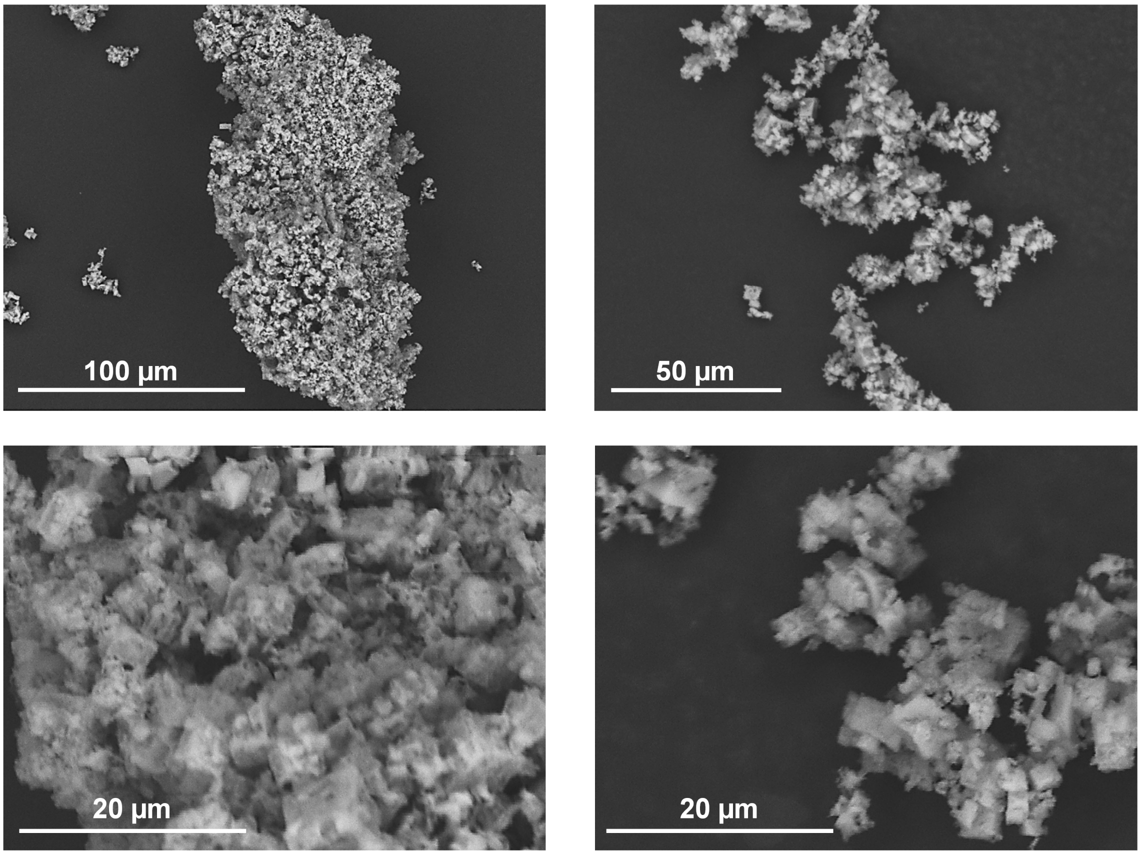

Figure S13. SEM micrographs at different magnifications (from top to bottom, and to the left to the right: 1000, 1500, 5000 and 5000) and of different zones of the sample highly-interpenetrated MOF-5 prepared at room temperature using Na_2BDC as linker source.

References

(1) Loiseau, T.; Serre, C.; Huguenard, C.; Fink, G.; Taulelle, F.; Henry, M.; Bataille, T.; Ferey, G. *Chem. Eur. J.* **2004**, *10*, 1373.
(2) Ahnfeldt, T.; Gunzelmann, D.; Loiseau, T.; Hirsemann, D.; Senker, J.; Ferey, G.; Stock, N. *Inorg. Chem.* **2009**, *48*, 3057.
(3) Biswas, S.; Ahnfeldt, T.; Stock, N. *Inorg. Chem.* **2011**, *50*, 9518.
(4) Rosi, N. L.; Kim, J.; Eddaoudi, M.; Chen, B. L.; O'Keeffe, M.; Yaghi, O. M. *J. Am. Chem. Soc.* **2005**, *127*, 1504.

(5) Tranchemontagne, D. J.; Hunt, J. R.; Yaghi, O. M. *Tetrahedron* **2008**, *64*, 8553.
(6) Díaz-García, M.; Mayoral, Á.; Díaz, I.; Sánchez-Sánchez, M. *Crystal Growth Des.* **2014**, *14*, 2479.
(7) Eddaoudi, M.; Kim, J.; Rosi, N.; Vodak, D.; Wachter, J.; O'Keeffe, M.; Yaghi, O. M. *Science* **2002**, *295*, 469.
(8) Huang, L. M.; Wang, H. T.; Chen, J. X.; Wang, Z. B.; Sun, J. Y.; Zhao, D. Y.; Yan, Y. S. *Microporous Mesoporous Mater.* **2003**, *58*, 105.
(9) Calleja, G.; Botas, J. A.; Orcajo, M. G.; Sanchez-Sanchez, M. *J. Porous Mater.* **2010**, *17*, 91.
(10) Burton, A. W.; Ong, K.; Rea, T.; Chan, I. Y. *Microporous Mesoporous Mater.* **2009**, *117*, 75.
(11) Manjon-Sanz, A.; Sanchez-Sanchez, M.; Munoz-Gomez, P.; Garcia, R.; Sastre, E. *Microporous Mesoporous Mater.* **2010**, *131*, 331.
(12) Scherrer, P.; Gottingen, N. G. W. *Math-Pys. Kl.* **1918**, *2*, 96.
(13) Camblor, M. A.; Corma, A.; Valencia, S. *Microporous and Mesoporous Materials* **1998**, *25*, 59.
(14) Pourbaix, M. *Atlas of Electrochemical Equilibra in Aqueous Solution*; NACE International, Cebelcor: Huston, 1974.
(15) Botas, J. A.; Calleja, G.; Sanchez-Sanchez, M.; Orcajo, M. G. *Int. J. Hydrogen Energy* **2011**, *36*, 10834.
(16) Yang, H. M.; Song, X. L.; Yang, T. L.; Liang, Z. H.; Fan, C. M.; Hao, X. G. *RSC Adv.* **2014**, *4*, 15720.
(17) Zhao, Z. X.; Xia, Q. B.; Li, Z. *Sep. Sci. Technol.* **2011**, *46*, 1337.